Supplementary Material for "Three-dimensional surfactant-covered flows of thin liquid films on rotating cylinders"

Weihua Li and Satish Kumar

Department of Chemical Engineering and Materials Science, University of Minnesota, Minneapolis, MN 55455

In this supplementary material, we provide some details of the linear stability analyses that were carried out to investigate the influence of insoluble surfactant on the Rayleigh-Plateau (RP) instability and the Rayleigh-Taylor (RT) instability.

1 Rayleigh-Plateau instability

In the case where the cylinder is spinning so rapidly that gravitational forces are negligible, Eqs. (16) and (17) of the main text are the two coupled evolution equations that describe the variation of the film thickness and surfactant concentration. To gain insight into the growth of the axisymmetric RP instability, we neglect angular variations in film thickness and set $\partial h/\partial\theta = \partial^3 h/\theta^3\theta = 0$. With this assumption, Eqs. (16) and (17) of the main text become

$$(1+h)\frac{\partial h}{\partial t} = -\frac{1}{3}\frac{\partial}{\partial y}\left\{h^3\frac{\partial}{\partial y}\left(h+\frac{\partial^2 h}{\partial^2 y}\right)+h^3 S\frac{\partial h}{\partial y}\right\}+\frac{1}{2}Ma\frac{\partial}{\partial y}\left(h^2\frac{\partial h}{\partial y}\right), \quad (1)$$

$$r\frac{\partial \Gamma}{\partial t}+\frac{\partial}{\partial y}\left[\Gamma v_s\right] = \frac{1}{Pe}\frac{\partial}{\partial y}\left(r\frac{\partial \Gamma}{\partial y}\right), \quad (2)$$

where the surface velocity in the axial direction, v_s, is given by

$$v_s = \frac{1}{2}\left\{h^2\frac{\partial}{\partial y}\left(h+\frac{\partial^2 h}{\partial y}\right)+Sh^2\frac{\partial h}{\partial y}\right\}-Mah\frac{\partial \Gamma}{\partial y}. \quad (3)$$

In the case where surfactant has no influence on film evolution ($Ma = 0$), Eq. (1) reduces to that obtained by Evans *et al.* [1] for a surfactant-free axisymmetric film.

A standard normal mode decomposition is used for h and Γ,

$$\begin{aligned} h(x,y,t) &= H_b + H_0 \exp(ik_y y + st), \\ \Gamma(x,y,t) &= \Gamma_b + \Gamma_0 \exp(ik_y y + st), \end{aligned} \tag{4}$$

Substitution of the above equations into Eqs. (1) and (2) leads to an eigenvalue problem of the form

$$\mathbf{A} \begin{pmatrix} H_0 \\ \Gamma_0 \end{pmatrix} = s \begin{pmatrix} H_0 \\ \Gamma_0 \end{pmatrix}, \tag{5}$$

where

$$\mathbf{A} = \begin{pmatrix} \frac{H_b^3}{3r_b} k_y^2 [(1+S) - k_y^2] & -\frac{1}{2r_b} Ma k_y^2 H_b^2 \\ \frac{1}{2r_b} H_b^2 \Gamma_b k_y^2 [(1+S) - k_y^2] & -\frac{1}{r_b} \left(Ma H_b \Gamma_b k_y^2 + \frac{1}{Pe_s} r_b k_y^2 \right) \end{pmatrix}. \tag{6}$$

It is found that both roots are purely real, and only one of the roots becomes positive; it is this root shown in the results below.

As an example, we consider the case where $S = W^2 Bo = 0.09$, $H_b = 0.03162$, $\Gamma_b = 1$, and $Pe = 10^5$. We solve matrix equation (5) for three different values of Ma to yield growth rates of the RP instability, s_{RP}, as a function of wavenumber k_y. Results are shown in Fig. 1a.

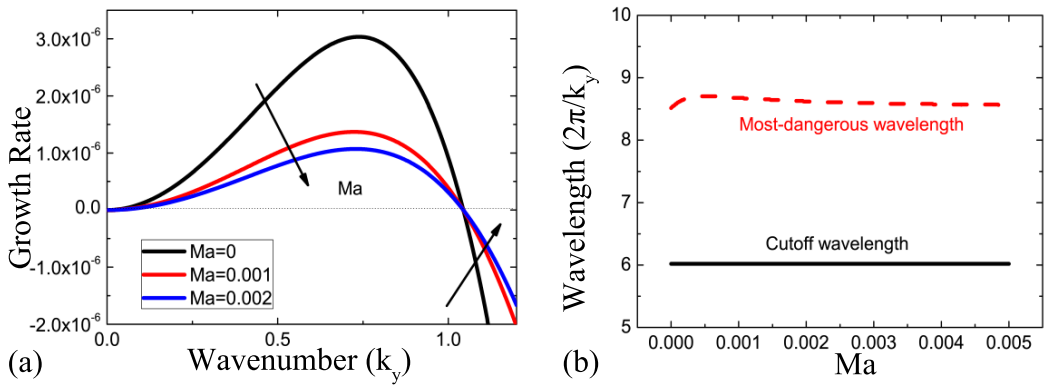

Figure 1: (a) Growth rates of the RP instability versus wavenumber for three different values of Ma with $S = 0.09$, $H_b = 0.03162$, $\Gamma_b = 1$, and $Pe = 10^5$. The arrows indicate the direction of increasing Marangoni number. (b) Corresponding most-dangerous wavelength (red dashed line) and cutoff wavelength (black solid line) of the RP instability versus Marangoni number.

Fig. 1a shows that the growth rate of the RP instability is positive over a range of wavenumbers (unstable region) and negative beyond the cutoff wavenumber (stable region). With an increase in the value of Ma, which corresponds to stronger Marangoni stresses, the value of s_{RP} decreases in the unstable region but increases in the stable region. This indicates that Marangoni stresses tend to suppress the growth rate of the RT instability, but hinder the leveling of perturbations to the film thickness. Similar behavior is also observed in the case where axial variations are neglected and perturbations can only grow in the angular direction [2]. The physical mechanisms responsible for the behavior observed in Fig. 1a are the same as those at play when purely angular perturbations are present [2].

We now investigate the evolution of the most-dangerous wavelength, $\lambda^{\star}_{\text{ring}} = 2\pi/k_y^{\max}$, for which the perturbation has the largest growth rate, and the cutoff wavelength, $\lambda_{\text{ring}} = 2\pi/k_y^{\text{cutoff}}$, for which the perturbation has a growth rate of zero. Here, $k_y^{\max}$ and k_y^{cutoff} are the corresponding most-dangerous wavenumber and cutoff wavenumber defined in the main text. Results are shown in Fig. 1b for $0 \leq Ma \leq 0.3$. In the surfactant-free case, the cutoff wavelength and the most-dangerous wavelength are $\lambda_{\text{ring}} = 2\pi/\sqrt{1+S} = 6.02$ and $\lambda^{\star}_{\text{ring}} = 2\sqrt{2}\pi/\sqrt{1+S} = 8.51$, respectively. Marangoni stresses have no influence on the cutoff wavelength (black solid line in Fig. 1b), and this is because at the cutoff wavelength, centrifugal forces are balanced by capillary forces and no Marangoni flows are present [2]. Marangoni stresses give rise to a slight increase (about 2%) in the value of the most-dangerous wavelength (red dashed line in Fig. 1b) in a small region near $Ma = 0$. However, with an increase in Ma (i.e., stronger Marangoni stresses), the value of $\lambda^{\star}_{\text{ring}}$ drops back to its value in the surfactant-free case. Similar behavior is observed for other parameter values.

2 Rayleigh-Taylor instability

In the case where the cylinder is stationary, the film on the cylinder tends to sag under the action of gravity, forming a ridge of liquid aligned with the cylinder axis at the cylinder bottom [3]. This ridge is unstable to gravity-induced axial perturbations, which is analogous to the Rayleigh-Taylor instability of a liquid layer underneath a horizontal flat plate.

To gain insight into the effects of surfactant on the RT instability, we consider a two-dimensional thin film of a Newtonian liquid laden with an insoluble surfactant underneath a horizontal plate (Fig. 2). Applying the lubrication approximation yields

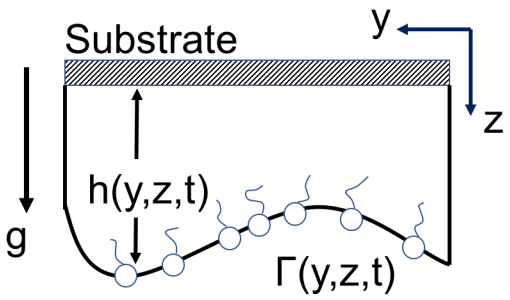

Figure 2: Schematic of problem geometry

the following dimensional evolution equations for the film thickness and surfactant surface concentration, respectively [1, 5]:

$$\frac{\partial h}{\partial t} = -\frac{\partial}{\partial y}\left\{\frac{h^3}{3\mu}\left[\frac{\partial}{\partial y}\left(\sigma\frac{\partial^2 h}{\partial y^2}\right) + \rho g\frac{\partial h}{\partial y}\right] - \varphi\frac{h^2}{2\mu}\frac{\partial \Gamma}{\partial y}\right\}, \tag{7}$$

$$\Gamma_t + (u_s\Gamma)_y = D\Gamma_{yy}, \tag{8}$$

where φ is the spreading pressure defined in the main text (§2.2) and u_s is the surface velocity at $z = h(y, z, t)$,

$$u_s = \frac{h^2}{2\mu}\frac{\partial}{\partial y}\left\{\sigma\frac{\partial^2 h}{\partial y^2} + \rho g h\right\} - \varphi\frac{h}{\mu}\frac{\partial \Gamma}{\partial y}. \tag{9}$$

To be consistent with Eqs. (1) and (2), we scale all lengths by R which can also be considered as the characteristic length scale along the film (y-direction). The resulting dimensionless evolution equations are

$$\frac{\partial h}{\partial t} = -\frac{\partial}{\partial y}\left\{\frac{h^3}{3}\left[Bo^{-1}\frac{\partial}{\partial y}\left(\frac{\partial^2 h}{\partial y^2}\right) + \frac{\partial h}{\partial y}\right] - Ma\frac{h^2}{2}\frac{\partial \Gamma}{\partial y}\right\}, \tag{10}$$

$$\Gamma_t + (u_s\Gamma)_y = Pe^{-1}\Gamma_{yy}, \tag{11}$$

where dimensionless constants Bo, Ma, and Pe are defined in the main text (Table 2).

After using a standard normal mode decomposition for h and Γ, we obtain a new matrix equation

$$\mathbf{A}\begin{pmatrix} H_0 \\ \Gamma_0 \end{pmatrix} = s\begin{pmatrix} H_0 \\ \Gamma_0 \end{pmatrix}, \tag{12}$$

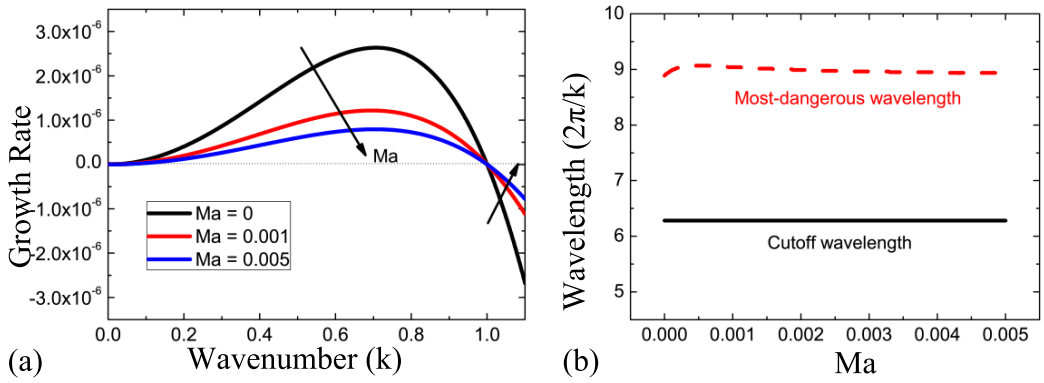

Figure 3: (a) Growth rates of the RT instability versus wavenumber for three different values of Ma with $Bo = 1$, $H_b = 0.03162$, $\Gamma_b = 1$, and $Pe = 10^5$. The arrows indicate the direction of increasing Marangoni number. (b) Corresponding most-dangerous wavelength (red dashed line) and cutoff wavelength (black solid line) of the RT instability versus Marangoni number

where

$$\mathbf{A} = \begin{pmatrix} \frac{1}{3}H_b^3[\frac{k^2}{Bo} - k^4] & -\frac{1}{2}MaH_b^2k^2 \\ \frac{1}{2}H_b^2\Gamma_b[\frac{k^2}{Bo} - k^4] & -(Ma\Gamma_b + \frac{1}{Pe})k^2 \end{pmatrix}. \tag{13}$$

As before, both roots are purely real, and only one of the roots becomes positive; it is this root shown in the results below.

As an example, we consider the case where $Bo = 0.01$, $H_b = 0.03162$, $\Gamma_b = 1$, and $Pe = 10^5$. We solve for growth rates of the RT instability, s_{RT}, as a function of wavenumber k. Results are shown in Fig. 3a for three different values of Ma. The most-dangerous wavelength, $\lambda^\star_{\text{drop}}$, and the cutoff wavelength, λ_{drop}, as functions of Ma are shown in Fig. 3b. We briefly summarize our findings.

Marangoni stresses tend to suppress the growth rate of the RT instability (Fig. 3a), similar to the RP-instability (Fig. 1a). With the presence of surfactant, the cutoff wavelength remains constant, $\lambda_{\text{drop}} = 2\pi/\sqrt{Bo} = 6.28$ (black solid line in Fig. 3b), while the value of the most-dangerous wavelength, $\lambda^\star_{\text{drop}}$, increases slightly (by about 2%) in a small region near $Ma = 0$ and drops back to its value in the surfactant-free case ($\lambda^\star_{\text{drop}} = 2\sqrt{2}\pi/\sqrt{Bo} = 8.89$) with an increase in Ma (red dashed line in Fig. 3b). Similar behavior is observed for other parameter values.

References

[1] P. L. Evans, L. W. Schwartz, and R. V. Roy. Three-dimensional solutions for coating flow on a rotating horizontal cylinder: Theory and experiment. *Physics of Fluids*, 17:072102, 2005.

[2] W. Li and S. Kumar. Thin-film coating of surfactant-laden liquids on rotating cylinders. *Physics of Fluids*, 27:072106, 2015.

[3] D. E. Weidner, L. W. Schwartz, and M. H. Eres. Simulation of coating layer evolution and drop formation on horizontal cylinders. *Journal of Colloid and Interface Science* 187: 243–258, 1997.

[4] B. Tsai, M. S. Carvalho, and S. Kumar. Leveling of thin films of colloidal suspensions. *Journal of Colloid and Interface Science*, 343:306–313, 2010.

[5] L. W. Schwartz, D. E. Weidner, and R. R. Eley. An analysis of the effect of surfactant on the leveling behavior of a thin liquid coating layer. *Langmuir*, 11:3690–3693, 1995.